

## Research Article

# Nanoparticles Containing Anti-inflammatory Agents as Chemotherapy Adjuvants: Optimization and *In Vitro* Characterization

Xiuling Lu,<sup>1,3</sup> Melissa D. Howard,<sup>1</sup> Marta Mazik,<sup>1</sup> Joshua Eldridge,<sup>1</sup> John J. Rinehart,<sup>2</sup> Michael Jay,<sup>1</sup> and Markos Leggas<sup>1</sup>

Received 5 December 2007; accepted 28 January 2008; published online 4 March 2008

**Abstract.** The pre-administration of dexamethasone (DEX) has previously been shown to enhance the anti-tumor efficacy of chemotherapeutic agents. The delivery of anti-inflammatory agents specifically to tumors via nanoparticle carriers is expected to promote the effectiveness of chemotherapeutic agents while avoiding systemic toxicities. The process for preparing solid lipid nanoparticles containing anti-inflammatory agents using the nanotemplate engineering method was optimized. Due to the solubilization of DEX in the bulk aqueous phase, its more lipophilic palmitate ester was synthesized and incorporated in nanoparticles that included a pegylating agent, PEG6000 mono-stearate, as part of the formulation. The stealth properties of these nanoparticles were demonstrated to be enhanced compared to latex particles by measuring the adsorption of radioiodinated IgG (185  $\mu\text{g}$  vs. 6.7  $\mu\text{g}$  IgG/mg NP). In addition, the uptake of  $^{14}\text{C}$ -labeled nanoparticles by murine macrophages was shown to decrease from 36.6% to 14.7% of the nanoparticles/mg cell protein as the amount of pegylating agent in the formulation increased from 0 to 4 mg/mL. The high loading values and low burst effect observed for these DEX palmitate-containing nanoparticles in addition to their stealth properties are expected to allow for the delivery of sufficient amounts of DEX to tumors to enhance the uptake of chemotherapeutic agents.

**KEY WORDS:** adsorption; biodegradable; dexamethasone; macrophage; microemulsion; nanoparticle; tumor.

## INTRODUCTION

Many anticancer agents exhibit lower efficacy and greater toxicity *in vivo* than *in vitro*. This discrepancy may be attributed to *in vivo* physiologic drug resistance due to the abnormal tumor tissue microenvironment (1,2). The aberrant tumor microenvironment is characterized by increased interstitial fluid pressure, fluid volume, and protein deposition, all of which might limit drug penetration into the tumor and a phenomenological resistance phenotype (3). The molecular events associated with these physiological changes are linked to cytokines released by cells of the innate immune response to the tumor and by tumor cells. In addition, cytokines released by tumor-associated macrophages enhance tumor proliferation, metastasis and invasion, and promote angiogenesis (4–7). In preclinical studies and two clinical trials, we have demonstrated that dexamethasone (DEX) administered immediately prior to chemotherapy increases the effectiveness of chemotherapy and decreases toxicity (8–11). The molecular mechanisms medi-

ating these observations may involve DEX down-regulation of nuclear factor-kappa B (NF- $\kappa$ B) induced pro-oncogenic signals and pro-inflammatory cytokines (12–16). However, systemic DEX administration induces clinical toxicities, most notably immunosuppression by T-cell depletion and inhibition (17,18). As depicted in Fig. 1, delivery of DEX or other anti-inflammatory agents specifically to tumors via a nanoparticle carrier would be expected to promote the effectiveness of chemotherapeutic agents while avoiding the systemic toxicities of DEX administration.

One of the hallmarks of many tumors is a leaky endothelium. It has been reported that the inter-endothelial pore size in most tumor capillaries and venules is between 380 and 780 nm and, as such, long-circulating vectors between 100 and 300 nm would be expected to readily pass through these pores and accumulate in tumor tissue (19).

Coupled with the absence of lymphatic drainage from the tumors, higher concentrations of drug can accumulate in tumors (20). This effect is commonly referred to as the enhanced vascular permeability and retention (EPR) effect and is a direct result of the disorganized and rapid neo-vascularization process occurring in tumors. In addition, nanoscale particles are typically cleared from the systemic circulation via the reticuloendothelial system which is highly concentrated in cells associated with the innate immune response. Here we report on the development of nanoparticle formulations for the enhanced delivery of anti-inflammatory

<sup>1</sup>Department of Pharmaceutical Sciences, University of Kentucky, Lexington, Kentucky 40536-0082, USA.

<sup>2</sup>Department of Medicine, University of Kentucky, Lexington, Kentucky, 40536-0093, USA.

<sup>3</sup>To whom correspondence should be addressed. (e-mail: xiuling.lu@uky.edu)

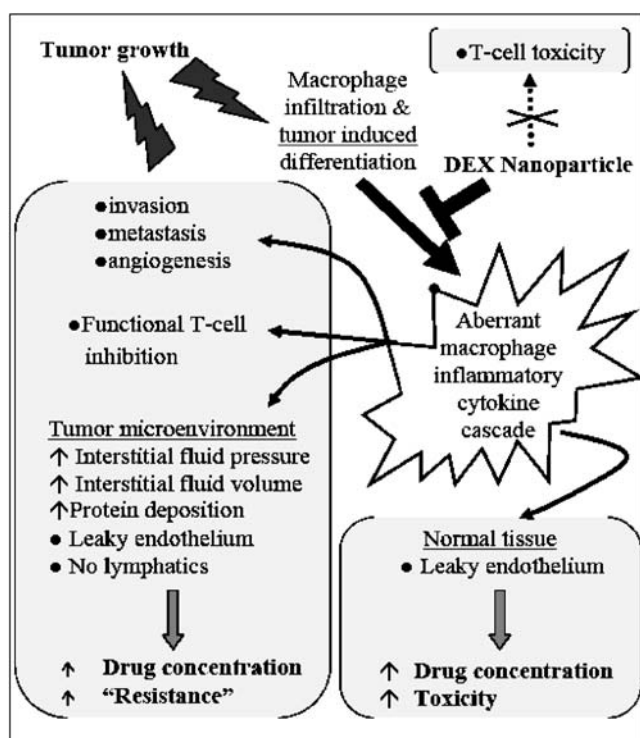


**Fig. 1.** A theoretical model depicting the role of dexamethasone (DEX) delivered via a nanoparticle carrier in blocking immune and cytokine related effects in the tumor microenvironment and in normal tissues

steroids to tumors, while minimizing drug exposure and toxicity in normal tissues.

Poly(lactic acid)-poly(glycolic acid) (PLGA) microspheres loaded with DEX have been developed to diminish the possibility of dose dumping, reduce the frequency of administration, and, therefore, increase patient compliance. The PLGA microspheres can be prepared by an oil-in-water (o/w) emulsion/solvent evaporation technique. However, there are some challenges with this approach. For example, this technique tends to produce larger particles in the range of 200 nm–15  $\mu$ m (21,22). Furthermore, it often requires the use of organic solvents like dichloromethane, and the *in vivo* degradation rate is slow. PLGA nanoparticles containing DEX have been reported (23) as have PLGA-DEX nanoparticles dispersed in alginate (24) and dextran (25) hydrogels. DEX-containing nanoparticles composed of block co-polymers have also been described (26). Liposome-incorporated corticosteroids were reported to inhibit certain types of inflammation in man and animals more intensely than a corresponding dose of free drug (27).

The manufacturing processes for preparing most nanoparticle drug delivery systems involve microfluidization, high-pressure homogenization and/or extrusion steps that are not always readily scalable. We have developed a process referred to as ‘nanotemplate engineering’ as an inexpensive, reproducible, and scalable nanoparticle formation process that avoids some of the issues associated with the preparation of other nanocarrier systems (28,29). This involves formation of a microemulsion precursor at elevated temperatures which, upon cooling, yields a suspension of solid nanoparticles. The current work describes the use of the nanotemplate engineer-

ing process to prepare solid lipid nanoparticles (NPs) containing anti-inflammatory agents. The process was optimized for maximum drug entrapment and stability, the release of the agents from the NPs was measured, and their stealth properties were assessed using two *in vitro* methods.

## MATERIALS AND METHODS

### Reagents

Emulsifying Wax NF, polysorbate 60 and Brij 78® were obtained from Uniqema, (Chicago, IL). DEX (USP) was a gift from Pfizer (Kalamazoo, MI). Betamethasone dipropionate (USP) was purchased from Spectrum (Gardena, CA). Tritiated DEX([6,7-<sup>3</sup>H(N)]; specific activity = 35–50 Ci/mmol) was purchased from American Radiolabeled Chemicals (Saint Louis, MO). PEG6000 mono-stearate (PEG6000 MS) was a gift from Stepan (Northfield, IL). Sodium [<sup>125</sup>I] iodide was purchased from Perkin-Elmer (Shelton, CT). Iodogen reagent was purchased from Pierce Biotechnology (Rockford, IL). Human IgG was purchased from Sigma-Aldrich (Saint Louis, MO). Latex particles (90 nm) were obtained from Ted Pella, Inc. (Redding, CA). Mouse plasma was purchased from Innovative Research, Inc. (Novi, MI) with sodium heparin as the anticoagulant. A murine macrophage cell line Raw 264.7 was purchased from ATCC (Manassas, VA) and cultivated using RPMI 1640 medium (Gibco, BRL). All the other chemicals were purchased from Sigma-Aldrich.

### Preparation of Nanoparticles: Selection of Components

The method to produce nanoparticles by the nanotemplate engineering approach has been previously described (28,29). Briefly, a microemulsion is formed by melting a matrix material (oil phase) and combining it with an appropriate mixture of water and surfactants. Hydrophobic drugs can be solubilized in the oil phase which, upon cooling of the microemulsion to room temperature, forms a suspension of solid NPs. The process usually employs a combination of Brij78® and Emulsifying Wax NF in a mass ratio of 1.75:1 and may include pegylating agents. Emulsifying Wax NF is a monograph material that is composed of cetyl-stearyl alcohol and polysorbate 60. In order to more finely control the composition of a formulation that would be optimal for the incorporation of DEX, a series of formulations was prepared in which combinations of cetyl alcohol, stearyl alcohol, Brij78®, various polysorbates and water as well as other components such as Cremophor RH, lecithin, and pegylating agents were used to prepare non-drug containing (blank) NPs by the nanotemplate engineering method. These preparations were initially characterized by their ability to form a stable microemulsion and by the particle size and polydispersity index (P.I.) seen with photon correlation spectroscopy. This was measured by scattering light at 90° (N4 Submicron Particle Sizer, Beckman Coulter Corporation, Miami, FL). Prior to the particle size measurement, the nanoparticles were diluted (1:30 v/v) with filtered water (0.22  $\mu$ m filter, Nalgene International) to ensure that the light scattering signal as indicated by the particle counts per second was within the sensitivity range of the instrument.

### Preparation of DEX-Loaded and Betamethasone Dipropionate-Loaded Nanoparticles

Initial attempts to prepare DEX-loaded NPs included efforts to dissolve DEX directly into the melted oil phase of the microemulsion. The solubility of DEX in various melted matrix materials was measured, and attempts to increase the solubilization of DEX in the melted oil phase included pre-dissolving DEX in solvents (e.g., acetone) and various melted surfactants, and increasing the ratio of oil:water in the microemulsion. The amount of DEX loading in the NPs was determined by using a validated HPLC method. Nanoparticle suspensions were ultrafiltered (CentriPlus, Millipore 100 kD) and subsequently dissolved in methanol prior to assaying. The DEX concentration in the filtrate and in the dissolved NPs was determined by HPLC (Alltech C18 column 5  $\mu$ m, 250 mm $\times$ 4.6 mm; acetonitrile: water (45:55) at 1 mL/min; 10  $\mu$ L injection; UV detection;  $\lambda$ =240 nm). This method was similarly used to assess the *in vitro* release of DEX from the NPs. These release studies were conducted by diluting the NPs in phosphate-buffered saline (PBS) buffer under sink condition and incubating the mixture at 37°C. A 0.5 mL sample was immediately withdrawn and the DEX content was determined by ultrafiltration and HPLC as described above. Additional samples were withdrawn over a 24 h period and similarly analyzed for DEX. In a similar manner, the solubility of betamethasone dipropionate (BD), an ester of a closely related steroid, was measured in various melted matrix materials and surfactants, and a number of formulations were investigated to prepare BD loaded nanoparticles.

### Synthesis of Dexamethasone Palmitate (DEX-P)

Dexamethasone palmitate (DEX-P) was synthesized using a modification of reported methods (30–32). Briefly, 300 mg of DEX was dissolved in 12 mL pyridine after which 578 mg of palmitoyl chloride was added drop wise. The mixture was allowed to stir in the dark under nitrogen for 24 h. The solvent was removed by nitrogen and the product was dissolved in dichloromethane before loading onto a 30 mL silica gel column. Elution of the column with a dichloromethane to dichloromethane:ethyl acetate (6:4 v/v) gradient was used to isolate the purified product. Progress of the reaction was monitored by silica gel thin layer chromatography (TLC) with chloroform:ethyl acetate (7:3) as the mobile phase. Retention factor (33) values were 0.10 and 0.69, for DEX and DEX-P, respectively. Product purity was determined by reverse phase HPLC using an assay similar to that described above for DEX, except that the mobile phase consisted of acetonitrile:water in a 95:5 ratio and the flow rate was 2 mL/min. The retention time of DEX-P in this system was 12 min. The structure of the product was confirmed by NMR (GEMINI-200, <sup>1</sup>H 199.9 MHz, <sup>13</sup>C 50.2 MHz) and mass spectrometry (+EI/direct probe, ThermoFinnigan Polaris).

### Synthesis of <sup>3</sup>H-DEX-P

An ethanolic solution containing 5 mg of DEX and 250  $\mu$ Ci of <sup>3</sup>H-DEX was prepared. The ethanol was evaporated followed by the addition of 0.5 mL pyridine and

9 mg of palmitoyl chloride. The product was isolated using the gradient elution system described for the unlabeled product, and purity was determined by TLC and liquid scintillation counting (LSC; Packard TRI-CARB® 2200CA)

### Preparation of DEX-Palmitate Nanoparticles

Microemulsions comprised of stearyl alcohol (1.6 mg/mL), polysorbate 60 (0.4 mg/mL), Brij78® (2.8 mg/mL) and PEG6000 MS (2.5 mg/mL) were prepared in which the amount of DEX-P added to the melted oil phase varied from 10–30% of the weight of the stearyl alcohol. The resulting particle sizes were measured at 25°C using a Coulter N4 Plus Submicron Particle Sizer. The results were confirmed by transmission electron microscopy (TEM) at 43,000 $\times$  magnification. A drop of nanoparticle suspension was deposited on a copper mesh carbon-coated grid and allowed to settle for 1 min at room temperature. After removal of excess fluid, the sample was negatively stained using 2% uranyl acetate for 1 min at room temperature. The excess uranyl acetate was removed and the grid was air-dried before obtaining the TEM image (Philips Tecnai Biotwin 12 with a Gatar digital camera; 100 kV). The amount of DEX-P incorporated into the NPs was determined by using the validated method in which the nanoparticle suspensions were ultrafiltered (100 kD) and subsequently dissolved in methanol. The DEX concentration in the filtrate and in the dissolved NPs was determined by HPLC as described above. The stability of these NP suspensions in terms of particle size after storage at 4°C was assessed by analyzing samples at specified time points over an 8-week period.

### Release of DEX-P from NPs

A suspension of NPs (20  $\mu$ L) was prepared in which either <sup>14</sup>C-stearyl alcohol or <sup>3</sup>H-DEX-P had been incorporated into the nanoparticle matrix and subsequently purified by gel permeation chromatography (GPC). The immediate release of the radiolabels from the NPs was measured by ultrafiltration (100 kD) and the radioactivity in the filtrate was quantified by LSC. The release of the radiolabels from the <sup>14</sup>C-nanoparticle or <sup>3</sup>H-DEX-P NP suspensions in plasma over time was measured by adding 20  $\mu$ L of the nanoparticle suspension and 280  $\mu$ L of 10% mouse plasma to a 100 kD Spectrum float dialysis membrane and placing it in 20 mL of 10% plasma at 37°C with stirring. At each time point, 1 mL of the dialysate was removed for assay by LSC and was replaced by 1 mL of fresh 10% plasma. After 24 h, the entire 20 mL dialysate was replaced with fresh 10% plasma. The release of <sup>3</sup>H-DEX-P from the NPs in PBS buffer containing 0.02% Tween 80 was measured in a manner similar to its release in 10% plasma, including the maintenance of sink conditions. TLC was used to detect the % of <sup>3</sup>H-DEX-P and <sup>3</sup>H-DEX retained in the NPs or released into the medium.

### Stealth Properties of Pegylated DEX-P NPs

Four batches of radiolabeled NPs were prepared in which a portion of the surfactant was replaced with a pegylating agent. The formulations contained 1.6 mg/mL of

stearyl alcohol (including 3.5  $\mu\text{Ci/mL}$  of  $^{14}\text{C}$ -stearyl alcohol), 0.4 mg/mL of polysorbate 60, 2.8 mg/mL of Brij78®, and PEG6000 MS at a concentration ranging from 0–4.0 mg/mL. The pegylating agent was incorporated into the NPs by adding the reagent to a mixture of melted stearyl alcohol, polysorbate 60 and Brij78® as the microemulsion was being formed. The stealth properties of these NPs were assessed *in vitro* by measuring the amount of IgG that adsorbed onto the NPs.  $^{125}\text{I}$ -labeled IgG was prepared using the Iodogen reagent and purified by GPC.  $^{125}\text{I}$ -labeled IgG was mixed with unlabeled IgG and the final concentration of IgG used in these experiments was 2.5 mg/mL. Latex particles (90 nm) were used as a positive control. After exposure of the particle suspensions to  $^{125}\text{I}$ -IgG for 60 min at 37°C, the mixture was passed through a GPC column (Sephadex CL-4B) to separate the  $^{125}\text{I}$ -IgG bound to the NPs from unbound  $^{125}\text{I}$ -IgG. A murine macrophage cell line (Raw 264.7) was employed to study the phagocytic uptake of nanoparticles; the cells were grown in monolayer in RPMI 1640 medium supplemented with 10% fetal bovine serum at 37°C and 5%  $\text{CO}_2$ . For quantification of phagocytosis, approximately  $5 \times 10^5$  cells were incubated for 24 h at 37°C in a 24-well culture plate. Ten microliters of the stealth or non-stealth radiolabeled nanoparticle suspension (3.5  $\mu\text{Ci/mL}$ ) were added and, following an incubation period of up to 90 min, the cells were washed and rinsed twice with PBS buffer to remove the non-phagocytized NPs. The cells were lysed by addition of 0.5 mL of 0.5 M NaOH and 10 min of mixing on a rocker plate. Four hundred microliters of the cell lysate were added to a scintillation vial and the remainder ( $\sim 100 \mu\text{L}$ ) was saved to measure the protein concentration using the Lowry method. The cell lysate was acidified by adding 500  $\mu\text{L}$  of 1 M acetic acid and then added to 10 mL of cocktail for liquid scintillation counting. The results were expressed as percentage of the NPs taken up by the macrophages per milligram of cell protein.

### Statistical Analysis

Data are presented as mean  $\pm$  standard deviation. Groups were compared using analysis of variance (ANOVA), one-way or two-way tests as appropriate, with SigmaStat 3.11 software (Systat Inc., San Jose, CA). Differences were considered statistically significant when  $P < 0.05$ , and the Holm–Sidak method was used to perform pairwise multiple comparisons on significant effects and interactions.

## RESULTS AND DISCUSSION

The nanotemplate engineering technology is based on the entropy-driven and spontaneous formation of a microemulsion that can easily be used as a nanotemplate to form NPs from the dispersed droplet phase. The engineering process involves melting a pharmaceutically-acceptable matrix material at 60–70°C and forming a slurry of the melted material in water under minimal stirring. Upon the addition of defined amounts of a suitable pharmaceutically-acceptable polymeric surfactant, a clear and stable liquid matrix oil-in-water microemulsion is formed. Simple cooling of the heated microemulsion results in the formation of stable NPs that are typically less than 100 nm.

Ideally, solid NPs can be engineered within minutes in one vessel from these natural nanotemplates.

### Selection of Nanoparticle Formulation Components

Approximately 160 formulations containing various combinations of cetyl alcohol, stearyl alcohol, polysorbate 20, 40, 60 or 80, Brij78® (including some that contained no Brij78®), and others that contained Cremophor, lecithin and pegylating agents were prepared. An optimized formulation in terms of particle size distribution that yielded clear and transparent nanoparticle suspensions was obtained using the nanotemplate engineering method. This formulation was comprised of stearyl alcohol (1.6 mg/mL), polysorbate 60 (0.4 mg/mL) and Brij78® (3.5 mg/mL) and yielded NPs with a mean diameter of 72.5 nm (P.I.=0.05). The formulation was also adjusted for the inclusion of a pegylating agent, PEG6000 MS. This is essentially a pegylated analog of a stearyl ( $\text{C}_{16}$ ) function. This is expected to be more compatible with the primary component of the microemulsion oil phase, stearyl alcohol, than other pegylating agents such as DSPE-PEG. Because the pegylating agent possesses its own inherent surfactant properties, the optimized formulation was obtained by reducing the concentration of Brij78® to 2.8 mg/mL when PEG6000 MS was included in the formulation.

### Preparation of Nanoparticles Loaded with DEX or Betamethasone Dipropionate

The log P of DEX in octanol/water is 1.772 and its water solubility at 25°C is 0.1 mg/mL. The solubility of DEX in the various melted oil phases was limited, ranging from 0.4 wt.% in glyceryl monostearate to 4.5 wt.% in the polysorbates (20, 40 and 60). The various attempts to load DEX into nanoparticles by the nanotemplate engineering method yielded a formulation that produced nanoparticles with an average diameter of 70 nm and a DEX loading of 3.5%. The release of DEX from the NPs in PBS exhibited a large burst which accounted for 45–55% of the original amount of DEX that was loaded into the NPs. When one considers the dose of nanoparticles required to achieve therapeutic levels after delivery to tumors as well as the large burst effect, it was decided that DEX did not possess the ideal characteristics for incorporation into the nanotemplate engineered nanoparticles. Thus, another anti-inflammatory agent that had a similar therapeutic profile to DEX but of lower water solubility, betamethasone dipropionate, was investigated.

Betamethasone is similar to DEX in structure, partition coefficient and biological activity. Its lipophilic ester betamethasone dipropionate, which is found in approved products, has a log P of 4.23 and a water solubility of 1.2 mg/L at pH 7.4 (25°C) (34). The solubility of betamethasone dipropionate in most tested melted matrices was 20–24%, which was much greater than that of DEX. A microemulsion in which betamethasone dipropionate was dissolved in a melted matrix was formed at 70°C, but upon cooling, the mixture turned very cloudy and the particle size was very large. Several attempts to modify the formulation did not result in the formation of a suitable nanoparticle suspension. Thus, our attention was turned to a more lipophilic derivative of DEX, i.e., its palmitate ester.



### Preparation of DEX Palmitate Nanoparticles

DEX-P has been used in marketed products such as Limethason®, an intravenously administered lipid emulsion. In a chronic inflammatory disease model, this product exhibited up to 5 times greater anti-inflammatory activity than DEX (35). A liposome formulation containing DEX-P has also been described and conformational analysis showed that the relatively hydrophilic portion of the molecule was oriented towards the aqueous phase while the palmitate function was aligned with the acyl chains of phospholipids (27). It is expected that DEX-P would align similarly when incorporated into the solid lipid NPs produced from a microemulsion precursor.

DEX-P was synthesized and purified. The structure of the product was confirmed by <sup>1</sup>H NMR and <sup>13</sup>C NMR, matching that reported by Zhang et al (36), and mass spectrometry (+EI/direct probe, ThermoFinnigan Polaris 6; C<sub>38</sub>H<sub>59</sub>FO<sub>6</sub>, calculated: 630.881, observed: 630.4299]. The purity of the compound based on HPLC and TLC was 99%. Studies were conducted to optimize the incorporation of DEX-P into the NPs in which the concentration of all components was held constant and the amount of DEX-P added to the oil phase of the microemulsion was 10–30% of the weight of the added stearyl alcohol. It was observed that higher encapsulation efficiencies were obtained when the concentration of PEG6000 MS was increased to 2.5 mg/mL for the nanoparticles containing DEX-P, possibly as a result of the surfactant-like properties of this pegylating agent. The TEM image of the DEX-P-containing nanoparticles is shown in Fig. 2. The mean particle size was approximately 90 nm with an apparently narrow size distribution. As can be seen in Table I, the extent of encapsulation of DEX-P in the NPs was

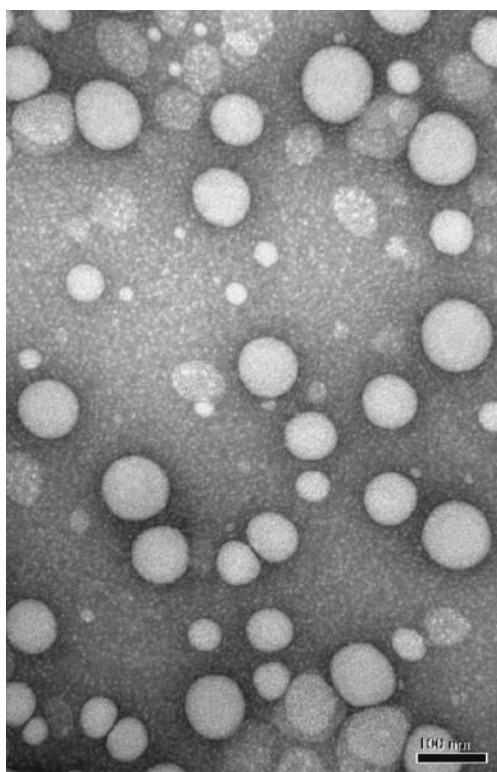


Fig. 2. TEM of pegylated DEX-P-containing nanoparticles

**Table I.** Characteristics of Nanoparticles Prepared from Stearyl Alcohol (1.6 mg/mL), Polysorbate 60 (0.4 mg/mL), Brij78® (2.8 mg/mL), PEG6000MS (2.5 mg/mL) and Dexamethasone Palmitate (DEX-P; 0.16–0.48 mg/mL). Particle Sizes are Described as the Mean ( $\pm$  std. dev.) of 3 Measurements

DEX-P <sup>a</sup>	10%	20%	30%
Particle size (nm)	88.4 $\pm$ 10.7	128.9 $\pm$ 17.4	132.2 $\pm$ 19.3
Polydispersity index	0.041	0.014	0.025
Encapsulation yield	94.1%	97.3%	92.1%

<sup>a</sup>DEX-P as percent of stearyl alcohol (w/w). Encapsulation yield= DEX-P in nanoparticles/DEX-P initially added  $\times$ 100%

>90% using the nanotemplate engineering method, even when large amounts of DEX-P were added to the microemulsion precursor, although particle size appeared to increase with increasing DEX-P.

The particle size of the 10% DEX-P loaded NPs was measured over an 8-week period when stored at 4°C. As can be seen in Fig. 3, the mean particle size gradually increased over time, likely as a result of Ostwald ripening (22). NPs prepared by the nanotemplate engineering method containing a variety of drugs have exhibited a similar Ostwald ripening effect that levels off at approximately 150 nm after 8–10 weeks of storage (22). These particles are expected to remain in the size range appropriate for tumor uptake by the EPR effect (1,2).

### Release of DEX Palmitate from Nanoparticles

In the studies using ultrafiltration to measure the release of the radiolabels from the NPs in PBS buffer, only 7% of the <sup>3</sup>H-DEX-P was found in the filtrate after 7 days. When the radiolabeled NPs were suspended in 10% plasma as opposed to PBS buffer, an initial burst (10%) of <sup>3</sup>H-DEX-P was observed. Figure 4 shows that after 12 h of incubation, approximately 65% of the radiolabel had been released from the NPs; this value reached 100% after 48 h. However, no burst release was observed with <sup>14</sup>C-stearyl alcohol in the dialysate, and the total amount released was much lower than observed for <sup>3</sup>H-DEX-P. Thus, it appeared that the release of DEX-P from the NPs was not due to the degradation of the particles, as this would have been expected to result in the

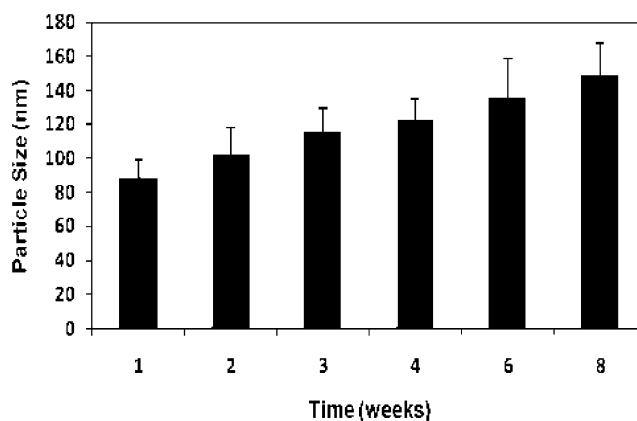
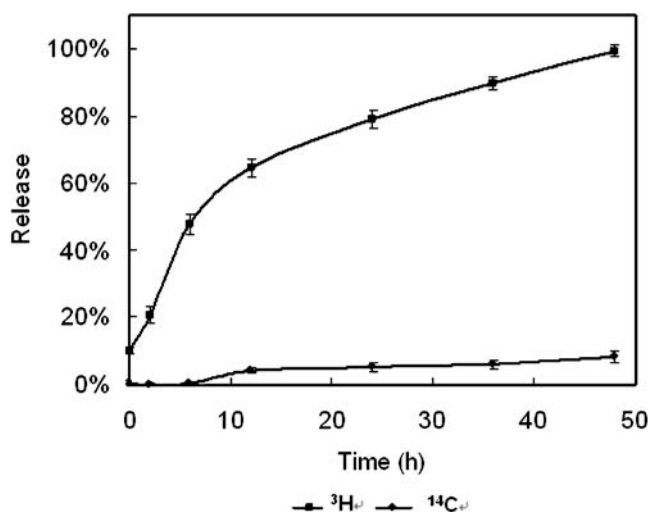


Fig. 3. Particle size of DEX-P nanoparticles following storage at 4°C. Mean ( $\pm$  std. dev.) of 3 measurements per time point



**Fig. 4.** <sup>3</sup>H-DEX-P and <sup>14</sup>C-Stearyl alcohol release from NPs in 10% plasma (37°C). Mean ( $\pm$  std. dev.) of 3 measurements per time point

release of greater amounts of <sup>14</sup>C-stearyl alcohol, a component of the nanoparticle matrix, into the dialysate. Either DEX-P was diffusing from the NPs or the ester was being hydrolyzed at the surface of the NP and releasing <sup>3</sup>H-DEX into the medium.

TLC analysis of the ultrafiltrates of the nanoparticle suspensions demonstrated that most of the radioactivity (<sup>3</sup>H) was present as intact DEX-P. However, the radioactive contents of the dialysates in the NP release studies in plasma revealed that >90% of the radioactivity (<sup>3</sup>H) was present as DEX, indicating that de-esterification of DEX-P had occurred. In separate experiments, it was demonstrated that when <sup>3</sup>H-DEX-P was incubated in 10% plasma at 37°C, 80% is converted to <sup>3</sup>H-DEX in 1 h. It is unclear if the <sup>3</sup>H-DEX-P is first released and then de-esterified, or if the de-esterification and subsequent release of <sup>3</sup>H-DEX into the medium drives the equilibrium toward greater release. The release of DEX reached 50% in 8 h, which was expected to provide adequate time for DEX-P NPs to circulate in plasma and accumulate in tumor tissue before DEX is released into the tumor.

### Stealth Properties of Pegylated DEX Palmitate Nanoparticles

The stealth properties of these NPs were evaluated by comparing the adsorption of <sup>125</sup>I-IgG to blank and non-pegylated DEX-P-containing NPs. Latex particles were used as a positive control, representative of a hydrophobic surface that would readily adsorb IgG. The results of the <sup>125</sup>I-IgG adsorption studies appear in Table II. These results showed that very little IgG was adsorbed to the NPs, even those that had not been pegylated, relative to the latex particles. This may be due to the presence of the Brij78® surfactant on the surface of the particles. The four groups were compared using the one-way ANOVA test,  $n=3$ . The differences in the mean values among the treatment groups are greater than would be expected by chance; there is a statistically significant difference ( $P<0.001$ ). Pairwise multiple comparisons (Holm-Sidak method) showed a statistically significant difference for

**Table II.** Adsorption of <sup>125</sup>I-IgG to Nanoparticles

Particles	$\mu\text{g IgG/mg NP}$
Latex	185.0 $\pm$ 9.5
Non-Pegylated Blank NPs	14.2 $\pm$ 1.3
Non-Pegylated DEX-P NPs	20.8 $\pm$ 1.6
Reduced Brij Dex NPs (2.5 mg/mL PEG6000 MS)	6.7 $\pm$ 0.7

Mean ( $\pm$  std. dev.) of 3 measurements.

the three nanoparticle groups *versus* control, latex particles ( $P<0.05$ ). Pegylated DEX-P NPs showed the least IgG adsorption, which was significantly different from that of the non-pegylated DEX-P NPs ( $P<0.05$ ).

The stealth properties of NPs that had been radiolabeled with <sup>14</sup>C-stearyl alcohol were also evaluated by their uptake by murine macrophages. The initial macrophage uptake studies were conducted using NPs prepared with the same concentration of PEG6000 MS as has been used in the IgG adsorption studies, i.e., 2.5 mg/mL. While there was a difference in the NPs taken up by these cells after a 90 min incubation compared to NPs that had been prepared without PEG6000 MS, the difference at earlier time points was not conclusive. Additional studies were performed to observe the effect of including higher concentrations of PEG in the preparation of the NPs on macrophage uptake of the NPs. The comparison is shown in Fig. 5. Two-way ANOVA revealed that the effect of different formulations depends on what time uptake was evaluated. There was a statistically significant interaction between formulation and time ( $P<0.001$ ). Multiple comparisons *versus* control group (non-pegylated nanoparticles) were done using the Holm-Sidak method. The pegylated nanoparticles significantly decreased the uptake of macrophage at the time points of 30, 60 and 90 min compared to the control group ( $P<0.05$ ). At the 90 min time point, each of the two groups was significantly different ( $P<0.05$ ). As more PEG6000 MS was used to formulate the NPs, the number of NPs taken up by the macrophages decreased. The uptake of <sup>14</sup>C-labeled nanoparticles by murine macrophages was 36.6%/mg cell

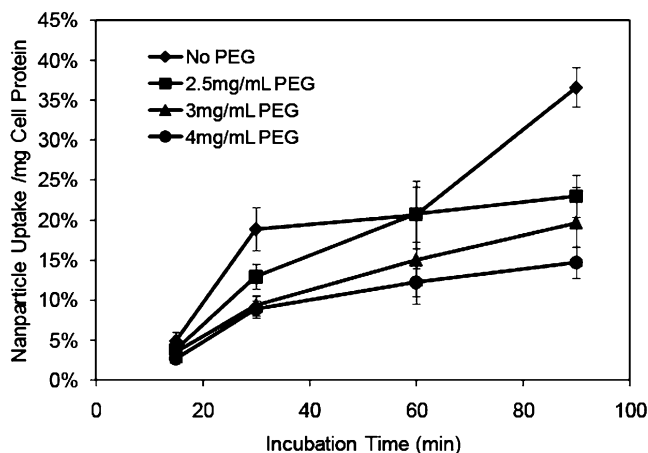


**Fig. 5.** Uptake of <sup>14</sup>C-labeled DEX-P nanoparticles by murine macrophages. Nanoparticles were formulated with varying amounts of PEG6000 MS and incubated for 15, 30, 60 and 90 min. Mean ( $\pm$  std. dev.) of 5 measurements per time point

protein for NPs containing no PEG6000 MS. As the amount of the pegylating agent in the formulation increased, the uptake of the <sup>14</sup>C-labeled nanoparticles was observed to decrease, reaching a low of 14.7%/mg cell protein for NPs formulated with 4 mg/mL of PEG6000 MS. These results indicated that as the degree of pegylation of the NPs increased, a corresponding increase in their stealth properties was imparted. The size of the NPs prepared with PEG6000 MS at a concentration of 4 mg/mL was 123 nm. As this was considered to be well within the acceptable range for tumor uptake via the EPR effect and increasing the amount of pegylating agent resulted in further increases in particle size, future studies evaluating stealth properties *in vivo* will be conducted with NPs formulated with PEG at a concentration of 4 mg/mL.

## CONCLUSION

The aim of this work was to use a readily scalable method of producing stable nanoparticles that could entrap an anti-inflammatory agent for the selective delivery of this agent to solid tumors. The components for the NPs were selected after exhaustive investigations to find the optimum composition. Attempts to incorporate DEX and betamethasone dipropionate, a more lipophilic analogue, into the NPs were not successful. However, the lipophilic palmitate ester of DEX was entrapped with high efficiency in the nanotemplate engineered NPs. A pegylating agent that was composed of a PEG derivative of stearyl alcohol, the primary component of the microemulsion oil phase, was included in the formulation in order to impart stealth properties to the resultant NPs. This is expected to enhance their retention in the circulation and increase their uptake in tumors via the EPR effect. The inclusion of PEG6000 MS in the formulation, which is itself a surface active agent that can aid in the stabilization of the microemulsion, allowed for the reduction of the concentration of the primary surfactant, Brij78®, in the final formulation. The stealth properties of these nanoparticles were demonstrated in *in vitro* tests of macrophage uptake and adsorption of radioiodinated IgG. Future studies evaluating stealth properties *in vivo* will be conducted with NPs formulated with PEG at a concentration of 4 mg/mL. It is anticipated that the stealth properties as well as the high loading values and low burst effect observed for these DEX-P nanoparticles will be adequate for the delivery of sufficient amounts of DEX to tumors to enhance the uptake of chemotherapeutic agents.

## ACKNOWLEDGMENTS

The authors are grateful for financial support from the Kentucky Cancer Experimental Therapeutics Program and Benedict Cassen Postdoctoral Fellowship from the Education and Research Foundation.

## REFERENCES

1. R. K. Jain. Transport of molecules in the tumor interstitium: a review. *Cancer Res.* **47**:3039–3051 (1987).
2. R. K. Jain. Delivery of molecular medicine to solid tumors. *Science* **271**:1079–1080 (1996).
3. C.-H. Heldin, K. Rubin, K. Pietras, and A. Ostman. High interstitial fluid pressure—an obstacle in cancer therapy. *Nat. Rev. Cancer* **4**:806–813 (2004).
4. F. Balkwill and A. Mantovani. Inflammation and cancer: back to Virchow? *Lancet* **357**:539–545 (2001).
5. L. M. Coussens and Z. Werb. Inflammation and cancer. *Nature* **420**:860–867 (2002).
6. G. Dranoff. Cytokines in cancer pathogenesis and cancer therapy. *Nat. Rev. Cancer* **4**:11–22 (2004).
7. M. M. Mueller and N. E. Fusenig. Friends or foes—bipolar effects of the tumour stroma in cancer. *Nat. Rev. Cancer* **4**:839–849 (2004).
8. J. Rinehart, L. Keville, J. Neiddhart, L. Wong, L. DiNunno, P. Kinney, M. Aberle, L. Tadlock, and G. Cloud. Hematopoietic protection by dexamethasone or Granulocyte-Macrophage Colony-Stimulating Factor (GM-CSF) in patients treated with carboplatin and ifosfamide. *Am. J. Clin. Oncol.* **26**:448–458 (2003).
9. J. J. Rinehart and L. R. Keville. Reduction in carboplatin hematopoietic toxicity in tumor bearing mice: comparative mechanisms and effects of interleukin-1 beta and corticosteroids. *Cancer Biother. Radiopharm.* **12**:101–109 (1997).
10. H. Wang, M. Li, J. J. Rinehart, and R. Zhang. Pretreatment with dexamethasone increases antitumor activity of carboplatin and gemcitabine in mice bearing human cancer xenografts: *in vivo* activity, pharmacokinetics, and clinical implications for cancer chemotherapy. *Clin. Cancer Res.* **10**:1633–1644 (2004).
11. H. Wang, M. Li, J. J. Rinehart, and R. Zhang. Dexamethasone as a chemoprotectant in cancer chemotherapy: hematoprotective effects and altered pharmacokinetics and tissue distribution of carboplatin and gemcitabine. *Cancer Chemother. Pharmacol.* **53**:459–467 (2004).
12. N. Auphan, J. A. DiDonato, C. Rosette, A. Helmberg, and M. Karin. Immunosuppression by Glucocorticoids: Inhibition of NF- $\kappa$ B Activity Through Induction of I $\kappa$ B Synthesis. *Science* **270**:286–290 (1995).
13. R. I. Scheinman, P. C. Cogswell, A. K. Lofquist, and J. A. S. Baldwin. Role of transcriptional activation of I $\kappa$ B alpha in mediation of Immunosuppression by glucocorticoids. *Science* **270**:283–286 (1995).
14. K. De Bosscher, W. Vanden Berghe, L. Vermeulen, S. Plaisance, E. Boone, and G. Haegeman. Glucocorticoids repress NF- $\kappa$ B-driven genes by disturbing the interaction of p65 with the basal transcription machinery, irrespective of coactivator levels in the cell. *Proc. Natl. Acad. Sci. U. S. A.* **97**:3919–3924 (2000).
15. Y. Yamamoto and R. B. Gaynor. Therapeutic potential of inhibition of the NF- $\kappa$ B pathway in the treatment of inflammation and cancer. *J. Clin. Invest.* **107**:135–142 (2001).
16. M. Grilli, J. J. Chiu, and M. J. Lenardo. NF- $\kappa$ B and Rel: participants in a multifunctional transcriptional regulatory system. *Int. Rev. Cytol.* **143**:1–62 (1993).
17. D. Franchimont, J. Galon, M. Gadina, R. Visconti, Y. J. Zhou, M. Aringer, D. M. Frucht, G. P. Chrousos, and J. J. O'Shea. Inhibition of Th1 immune response by glucocorticoids: dexamethasone selectively inhibits IL-12-induced stat4 phosphorylation in T lymphocytes. *J. Immunol.* **164**:1768–1774 (2000).
18. D. Franchimont. Overview of the actions of glucocorticoids on the immune response: a good model to characterize new pathways of immunosuppression for new treatment strategies. *Ann. N. Y. Acad. Sci.* **1024**:124–137 (2004).
19. S. K. Hobbs, W. L. Monsky, F. Yuan, W. G. Roberts, L. Griffith, V. P. Torchilin, and R. K. Jain. Regulation of transport pathways in tumor vessels: Role of tumor type and microenvironment. *Proc. Natl. Acad. Sci. U. S. A.* **95**:4607–4612 (1998).
20. R. Sinha, G. J. Kim, S. Nie, and D. M. Shin. Nanotechnology in cancer therapeutics: bioconjugated nanoparticles for drug delivery. *Mol. Cancer Ther.* **5**:1909–1917 (2006).
21. J. Panyam, D. Williams, A. Dash, D. Leslie-Pelecky, and V. Labhasetwar. Solid-state solubility influences encapsulation and release of hydrophobic drugs from PLGA/PLA nanoparticles. *J. Pharm. Sci.* **93**:1804–1814 (2004).
22. T. Hickey, D. Kreutzer, D. J. Burgess, and F. Moussy. Dexamethasone/PLGA microspheres for continuous delivery of an anti-inflammatory drug for implantable medical devices. *Biomaterials* **23**:1649–1656 (2002).

23. C. Gomez-Gaete, N. Tsapis, M. Besnard, A. Bochot, and E. Fattal. Encapsulation of dexamethasone into biodegradable polymeric nanoparticles. *Int. J. Pharm.* **331**:153–159 (2007).
24. D.-H. Kim and D. C. Martin. Sustained release of dexamethasone from hydrophilic matrices using PLGA nanoparticles for neural drug delivery. *Biomaterials* **27**:3031–3037 (2006).
25. M. G. Cascone, P. M. Pot, L. Lazzeri, and Z. Zhu. Release of dexamethasone from PLGA nanoparticles entrapped into dextran/poly(vinyl alcohol) hydrogels. *J. Mater. Sci. Mater. Med.* **13**:265–269 (2002).
26. Z. Zhang, D.W. Grijpma, and J. Feijen. Poly(trimethylene carbonate) and monomethoxy poly(ethylene glycol)-block-poly(trimethylene carbonate) nanoparticles for the controlled release of dexamethasone. *J. Control. Release* **111**:263–270 (2006).
27. H. Benameur, G. D. Gand, R. Brasseur, J. P. V. Vooren, and F. J. Legros. Liposome-incorporated dexamethasone palmitate: Chemical and physical properties. *Int. J. Pharm.* **89**:157–167 (1993).
28. R. J. Mumper, Z. Cui, and M. O. Oyewumi. Nanotemplate Engineering of Cell Specific Nanoparticles. *J. Dispers. Sci. Technol.* **24**:569–588 (2003).
29. M. O. Oyewumi, R. A. Yokel, M. Jay, T. Coakley, and R. J. Mumper. Comparison of cell uptake, biodistribution and tumor retention of folate-coated and PEG-coated gadolinium nanoparticles in tumor-bearing mice. *J. Control. Release* **95**:613–626 (2004).
30. Y. Mizushima, T. Hamano, and K. Yokoyama. Use of a lipid emulsion as a novel carrier for corticosteroids. *J. Pharm. Pharmacol.* **34**:49–50 (1982).
31. Y. Mizushima, T. Hamano, and K. Yokoyama. Tissue distribution and anti-inflammatory activity of corticosteroids incorporated in lipid emulsion. *Ann. Rheum. Dis.* **41**:263–267 (1982).
32. M. Teshima, S. Kawakami, K. Nishida, J. Nakamura, T. Sakaeda, H. Terazono, T. Kitahara, M. Nakashima, and H. Sasaki. Prednisolone retention in integrated liposomes by chemical approach and pharmaceutical approach. *J. Control. Release* **97**:211–218 (2004).
33. T. J. Harris, G. V. Maltzahn, A. M. Derfus, E. Ruoslahti, and S. N. Bhatia. Proteolytic actuation of nanoparticle self-assembly. *Angew. Chem. Int. Ed. Engl.* **45**:3161–3165 (2006).
34. L. Simonsen, G. Hoy, E. Didriksen, J. Persson, N. Melchior, and J. Hansen. Development of a new formulation combining calcipotriol and betamethasone dipropionate in an ointment vehicle. *Drug Dev. Ind. Pharm.* **30**:1095–102 (2004).
35. K. Yokoyama and M. Watanabe. Limethason as a lipid microsphere preparation: An overview. *Adv. Drug Deliv. Rev.* **20**:195–201 (1996).
36. H.Y. Zhang, M.J. Wu, J.J. Dong, J.G. Fu, T. Chen, and T.Z. Zhao. An NMR study of dexamethasone palmitate. *Chin. J. Magn. Reson.* **21**:405, 2004 (2004).